Supplementary Information

Two birds with one stone: A NIR fluorescent probe for mitochondrial proteins imaging and its application in photodynamic therapy

Ya-Lin Qi, [#] Long Guo, [#] Li-Li Chen, Dan-Dan Yuan, Hai-Rong Wang, Yu-Yao Cao, Yu-Shun Yang[*] and Hai-Liang Zhu[*]

State Key Laboratory of Pharmaceutical Biotechnology, School of Life Sciences, Nanjing University, Nanjing, 210023 (P. R. China)

Corresponding author: Yu-Shun Yang; E-mail: ys_yang@nju.edu.cn; Hai-Liang Zhu; E-mail: zhuhal@nju.edu.cn.

[#]These two authors made equal contributions.

Table of contents

1.1. The limit of detection (LOD) of MPP

The emission spectrum of free **MPP** in PBS buffer (10 mM, pH 7.4, containing 1% MeCN) was collected for 20 times to confirm the background noise σ. The linear regression curve was then fitted according to the data in the range of **MPP** from 0 to 10 mg/mL and the slope k was obtained. Afterwards, the limit of detection (LOD) was calculated using the following equation:

$$LOD = 3\sigma/k$$

Where σ is the standard deviation of eleven blank measurements, and k is the slope of the linear equation. The detection limit ($3\sigma/k$) was then determined to be 34.95 μg/mL (ca. 514.3 nM).

1.2. Determination of the fluorescence quantum yield

The fluorescence quantum yield **Φu** was estimated from the absorption and fluorescence spectra of **MPP** according to the equation, where using the ethanol solution of rhodamine B ($\Phi_s = 0.65$) for the reference[1]. The fluorescence quantum yield was calculated using equation as follows:

$$\Phi u = [(A_s F_u n^2)/ (A_u F_s n_0^2)]\ \Phi s$$

Φs is the quantum yield of reference substance; A_s and A_u represent the absorbance of the reference and testing solution at the excitation wavelength and controlled to be lower than 0.05 at the same time; F_s and F_u refer to the integrated emission band areas, n and n_0 are the solvent refractive indexes of sample and reference, respectively. **Φ** of **MPP** was 0.0034 and **Φ** of **MPP** with HSA was 0.024 ($\lambda_{ex} = 526$ nm).

1.3. TD-DFT calculation methods

The ground state structure of MPP was optimized at the B3LYP/6–311G (d) level using the Gaussian 16 package[2]. Then the excitation energies and the natural transition orbitals (NTOs) for electronic excited singlet and triplet states were calculated with the TD-DFT method. All calculations were conducted in solvent of water with the polarizable continuum model (PCM). At the same level, the spin orbital coupling (SOCs) between singlet and triplet states are calculated using the ORCA package.

1.4. Cell culture

HeLa (a human cervical carcinoma cell line) cells were cultured in Dulbecco's modified Eagle's medium (DMEM) and incubated under an atmosphere containing 5% CO_2 at 37 °C humidified air for 24 h. Here DMEM contains 10% fetal bovine serum and 1% penicillin-streptomycin.

1.5. Fluorescence imaging

The confocal fluorescent images were obtained with Zeiss LSM 980, Zeiss LSM 880 and Olympus FV1000 confocal microscopes. The co-localization experiments were imaged on a laser scanning confocal microscope (Olympus FV1000, 63 oil objective). The co-localization coefficient and mean fluorescence intensity of the images were determined by Image J and the software with Zeiss LSM 880.

1.6. The measurement of lipophilicity

Lipophilicity was presented as log Po/w values, which were determined by the flask-shaking method. An aliquot of a stock solution of the sample in aqueous NaCl (0.9% w/v and saturated with octanol) was added to an equal volume of octanol

(saturated with 0.9% NaCl, w/v), and the mixture was shaken overnight at 60 rpm to allow partitioning at 298 K. After the sample was centrifuged at 3000 rpm for 10 min, the probe content of the organic and aqueous phases was determined by UV absorbance (485 nm). Log P was then defined as the logarithmic ratio of probe concentrations in the organic and aqueous phases[3].

1.7. Evaluation of PDT efficacy in vitro

The dark and photo toxicities of **MPP** were evaluated against HeLa, MCF-7 and MCF-7 cells by 3-(4, 5-dimethylthiazol-2-yl)-2, 5-diphenyltetrazolium bromide (MTT) assay. For dark toxicities, HeLa, MCF-7 and MCF-7 cells were seeded in 96-well plates, separately. Subsequently, gradient concentrations of **MPP** (0 μM, 0.5 μM, 1 μM, 2 μM, 3 μM, 4 μM and 5 μM) were added into each well and co-cultured for 24 h. Afterwards, MTT (10 μL, 5 mg/mL in PBS) was added into each well. After the treatment for another 4 h, the supernatant was replaced by DMSO (100 μL) and the optical density (at 570 nm, referenced at 630 nm) was measured by a microplate reader. The cell viability (%) calculated as the survival cells after various treatments per nontreated cells.

As for photo toxicities, HeLa, MCF-7 and MCF-7 cells were seeded in 96-well plates, separately. Subsequently, gradient concentrations of **MPP** (0 μM, 0.5 μM, 1 μM, 2 μM, 3 μM, 4 μM and 5 μM) were added into each well and co-cultured for 24 h. After treatment for 4 h, the cells were irradiated with green light (17 w/m^2) for 10 min. An ice box was disposed below the 96-well plates to eliminate the influence of temperature. And then, MTT (10 μL, 5 mg/mL in PBS) was added into each well. After treatment for another 4 h, the supernatant was replaced by DMSO (100 μL) and the optical density (at 570 nm, referenced at 630 nm) was measured by a microplate reader. The cell viability (%) was again calculated as the survival cells after various treatments per nontreated cells.

Besides, the PDT therapeutic effects of **MPP** were also investigated against HeLa

cells by flow cytometry. Different concentration of **MPP** (0 μM, 0.5 μM, 1 μM, 2 μM, 3 μM, 4 μM and 5 μM) was co-cultured with HeLa cells for 24 h in 6-well plates. An ice box was disposed below the 6-well plates to eliminate the influence of temperature. Subsequently, the cells were irradiated with green light (17 w/m^2) for 0 min, 5 min and 10 min, respectively. The treated cells were then totally collected, centrifuged, and re-suspended in 390 μL of staining solution (containing 10 μL Annexin V-FITC and 20 mL PI in Binding Buffer), and then incubated for an additional 20 min at room temperature in dark. Samples were analyzed on an Attune NxT 4 flow cytometer (Thermo Fisher Scientific). FITC channel: excitation laser: 488 nm, emission filter: 500-600 nm; PI channel: excitation laser: 561 nm, emission filter: 605-635 nm.

1.8. Determination of singlet oxygen quantum yield (Φ_Δ)

The singlet oxygen quantum yield was determined by the reported method[4]. Rose Bengal (RB) as the standard photosensitizer and 1, 3-diphenylisobenzofuran (DPBF) was used as the singlet oxygen trapper. First, the concentration of DPBF in 3 mL water was modified to adjust the absorbance at 425 nm to be close to 1.0. Then, appropriate concentrations of RB and samples were added respectively to make sure that the absorbance of the mixture at 550 nm was between 0.2 and 0.3. After that, the mixture solutions were exposed to green light irradiation for 0-120 s and the absorption spectrum was recorded with a UV-vis spectrophotometer. At last, the singlet oxygen quantum yield was calculated with the following equation:

$$\Phi_\Delta = \Phi_{RB} \times (k_{(PS)} \times F_{(RB)}) / (k_{(RB)} \times F_{(PS)})$$

Φ_Δ represented the singlet oxygen quantum yield of the tested photosensitizer; Φ_{RB} represented the singlet oxygen quantum of RB and the value is 0.75 in water[5]; PS represented the tested photosensitizer **MPP**; k represented the slope of the decrease of the absorbance at 425 nm of DPBF with the addition of irradiation time; F was the correction factor which was calculated by the following equation:

$$F=1-10^{-OD}$$

OD represented the absorbance of the mixture at 550 nm.

1.9. Tumor mouse model

4-week-old female BALB/c nude mice were purchased from the Model Animal Research Centre of Nanjing University. All mice were maintained under specific pathogen-free conditions and used following the experimental animal guidelines set by the Institute of Animal Care and Use Committee. All animal experiments were approved by the Institutional Animal Care and Use Committee at Nanjing University. HeLa tumor cells (1.0×10^6 cells) resuspended in PBS (100 μL) were subcutaneously injected into the flanks of each mice. When the tumors reached approximate 60 mm³, the animals were subjected to the experiments. The tumor volumes were calculated using the following formula: tumor volume = the greatest longitudinal diameter (length) × the greatest transverse diameter (width)^2 ×0.5.

## 1.10. *In vivo* fluorescence imaging tumor

MPP (10 μM, 200 μL in PBS containing 1% MeCN) was administered through subcutaneous intratumoral injection. Then, the mice were anesthetized and imaged for 0 h, 0.5 h, 3 h, 6 h, 9 h and 24 h. In all the experiments mentioned in this paragraph, excitation filter of 535 nm and emission filter of DsRed (575-650 nm) were used. All imaging parameters were kept constant for the same mice model.

1.11. Histology examination

H&E staining was performed according to a method provided via the vendor (BBC Biochemical). After the experiments, the mice were sacrificed. The major organs (liver, lungs, kidneys, heart, and spleen) and tumor tissues from the mice in six groups were retrieved and cut into 4 μm sections, then fixed in a 10% paraformaldehyde solution for

8 h at room temperature, followed by the dehydration with ethanol and then processed routinely into paraffin. The sliced tissues were stained with H&E and examined by means of an inverted fluorescence microscope system (Nikon E 200).

2. Synthetic details, NMR spectra and HRMS spectra
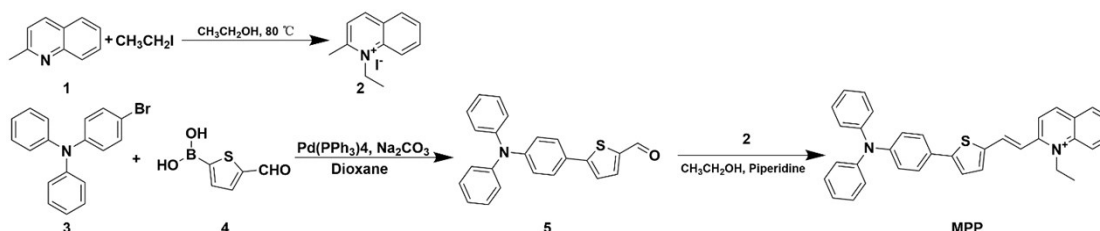
Synthesis of compound 2: The method was similar to our previously report[6]. 4-Methylquinoline (4.00 g, 28 mmol) was dissolved in ethanol (10 mL) and iodoethane (5.61g, 36 mmol) was added. The mixture stirred for 6 h at 80 °C in a sealed tube. The resulting solid was crushed, washed several times with ethyl ether and dried under vacuum to afford a green solid product without further purification. Yield: 4.80 g (50 %). ^{1}H NMR (400 MHz, DMSO-d_6) δ 9.12 (d, J = 8.6 Hz, 1H), 8.63 (d, J = 9.0 Hz, 1H), 8.43 (dd, J = 8.1, 1.3 Hz, 1H), 8.25 (ddd, J = 8.8, 7.0, 1.5 Hz, 1H), 8.14 (d, J = 8.6 Hz, 1H), 8.01 (t, J = 7.5 Hz, 1H), 5.01 (q, J = 7.2 Hz, 2H), 3.13 (s, 3H), 1.54 (t, J = 7.3 Hz, 3H). ^{13}C NMR (151 MHz, DMSO-d_6) δ 158.70 , 143.75 , 136.22 , 133.46 , 128.80 , 127.20 , 126.41 , 123.76 , 117.08 , 45.46 , 20.71 , 11.68 .

Synthesis of compound 5: Under a nitrogen atmosphere, 11 mmol (1.71 g) of (5-formylthiophen-2-yl) boronic acid and the 10 mmol (3.24 g) of 4-bromotriphenylamine compound were dissolved in 50 mL of dioxane. To the mixture 0.55 mmol of tetrakis (triphenylphosphine) palladium and 20 mmol of Na_2CO_3 (as 5 mL aqueos solution) were added. The whole reaction mixture was then refluxed with continuous stirring under the nitrogen atmosphere overnight. The reaction mixture was then cooled to room temperature and filtered. DCM (50 mL) and water (30 mL) were added to the filtrate, and shaken well. The organic layer was separated and dried over the MgSO4. The

solvent was evaporated under the reduced pressure and the crude was subjected to the column chromatography to obtain the pure yellow solid product. Yield: 0.99 g (20%). ^{1}H NMR (600 MHz,) δ 9.87 (s, 1H), 8.01 (d, J = 4.2 Hz, 1H), 7.70 (d, J = 9.1 Hz, 2H), 7.61 (d, J = 4.2 Hz, 1H), 7.36 (t, J = 8.2 Hz, 6H), 7.16 – 7.12 (m, 2H), 7.10 (d, J = 9.5 Hz, 7H), 6.97 (d, J = 9.1 Hz, 2H). ^{13}C NMR (101 MHz, DMSO-d_6) δ 184.08 , 148.99 , 146.88 , 141.35 , 139.86 , 130.20 , 127.85 , 126.01 , 125.41 , 124.53 , 124.40 , 122.18 .

Synthesis of MPP: A solution of compound **2** (149 mg, 0.419 mmol) and compound **5** (100 mg, 0.632 mmol) was refluxed under nitrogen in dry ethanol catalyzed by a few drops of piperidine overnight. After cooling to room temperature, the solvent was removed by evaporation under reduced pressure. The residue was purified using a neutral aluminum oxide column using a DCM and methanol mixture as the eluting solvent to give a dark powder of **MPP** (98 mg, 40 % of yield). ^{1}H NMR (600 MHz, Chloroform-d) δ 8.74 (dd, J = 21.2, 11.3 Hz, 3H), 8.20 (d, J = 8.8 Hz, 1H), 8.05 – 7.99 (m, 2H), 7.89 (d, J = 3.3 Hz, 1H), 7.70 (t, J = 7.4 Hz, 1H), 7.44 (d, J = 8.5 Hz, 2H), 7.34 (t, J = 7.9 Hz, 5H), 7.15 (dd, J = 15.4, 7.6 Hz, 9H), 7.04 (d, J = 8.6 Hz, 3H), 5.16 (d, J = 6.6 Hz, 2H), 1.27 (s, 3H). ^{13}C NMR (101 MHz, DMSO) δ 155.08, 150.54, 148.67, 146.92, 146.10, 143.92, 140.88, 138.58, 136.26, 135.75, 135.46, 131.12, 130.77, 130.25, 129.49, 129.22, 128.31, 127.50, 126.39, 126.03, 125.39, 125.12, 124.54, 122.37, 121.22, 119.30, 119.25, 115.70, 56.49, 19.04, 14.49. HRMS calculated 509.20, found 509.2044.
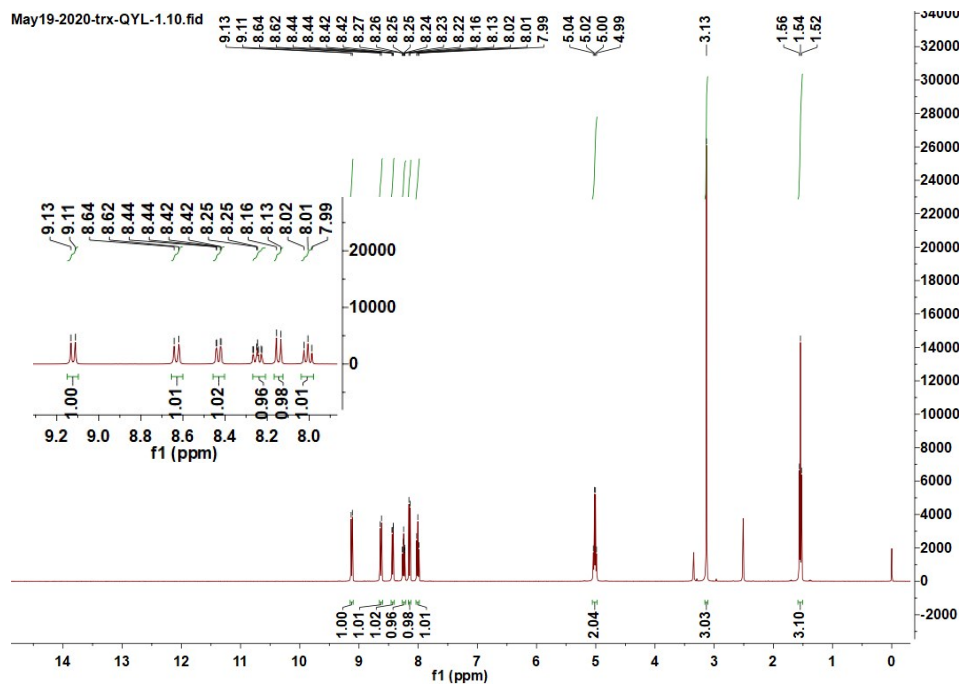
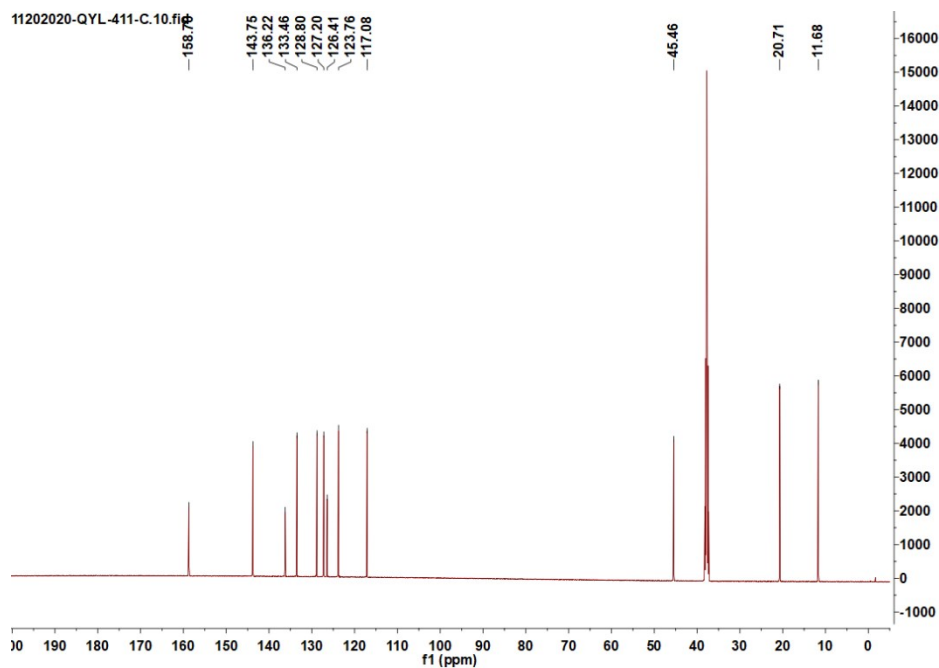**Fig. S1.** The ^{1}H NMR of compound **2** (400 MHz, in DMSO-d_6).

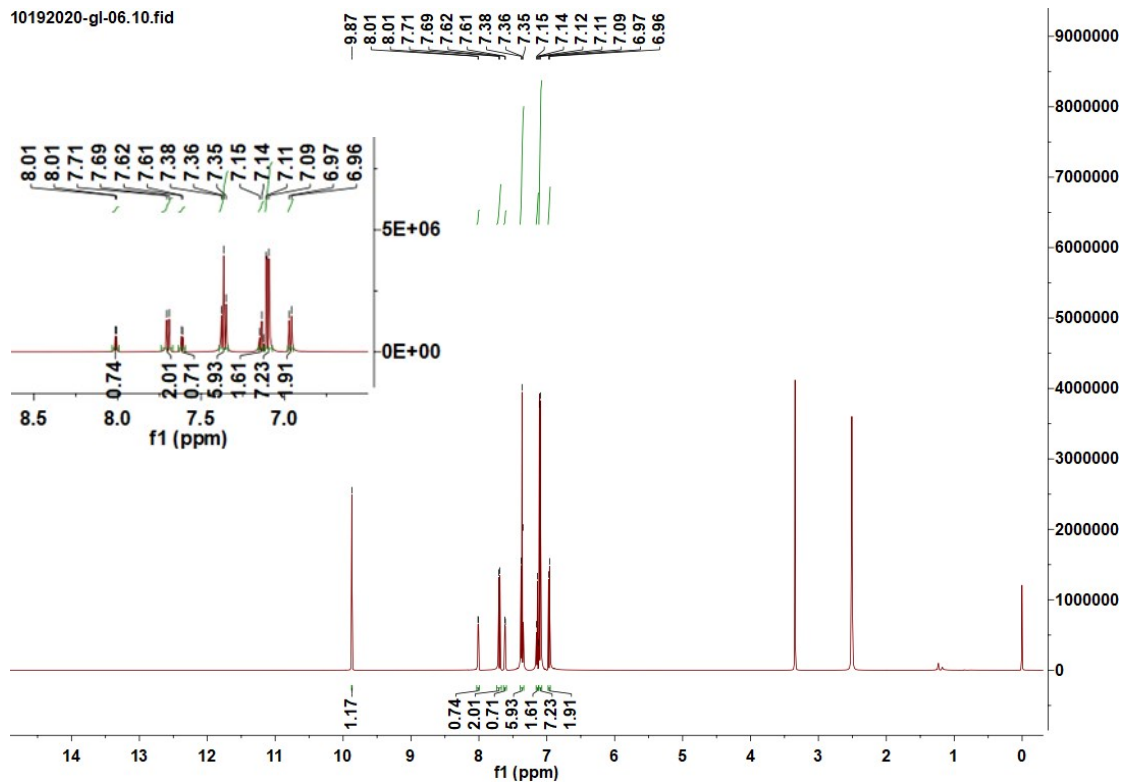**Fig. S2.** ^{13}C NMR of compound **2** (101 MHz, in DMSO-d_6).

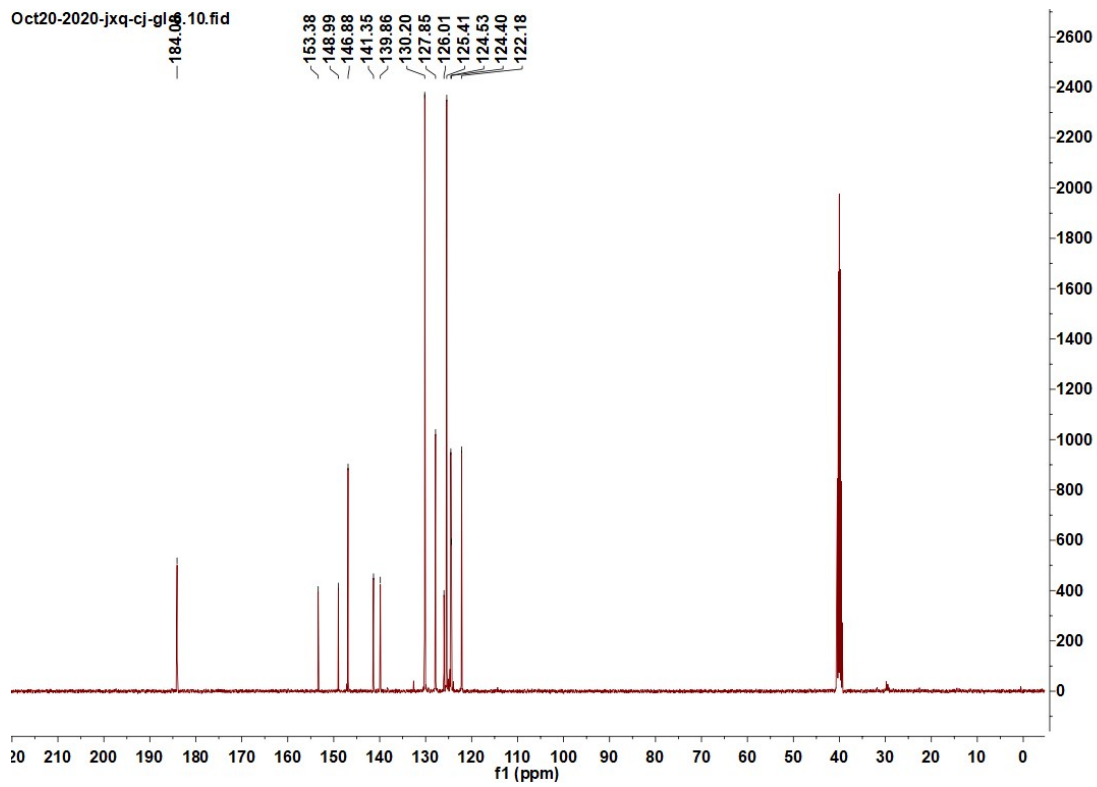**Fig. S3.** The ^{1}H NMR of compound **5** (600 MHz, in DMSO-d_6).

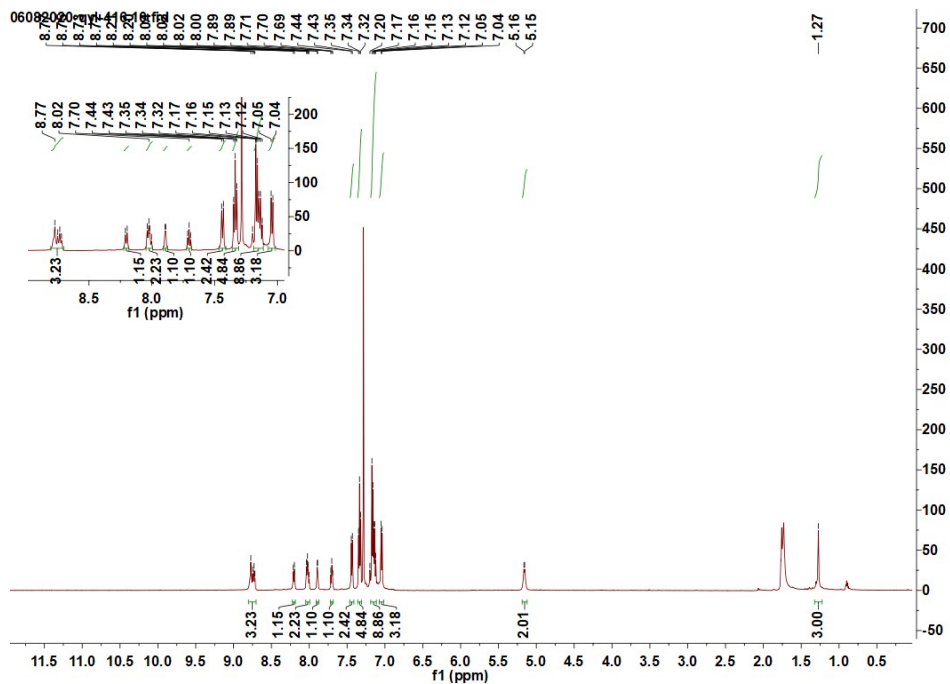**Fig. S4.** ^{13}C NMR of compound **5** (101 MHz, in DMSO-d_6).

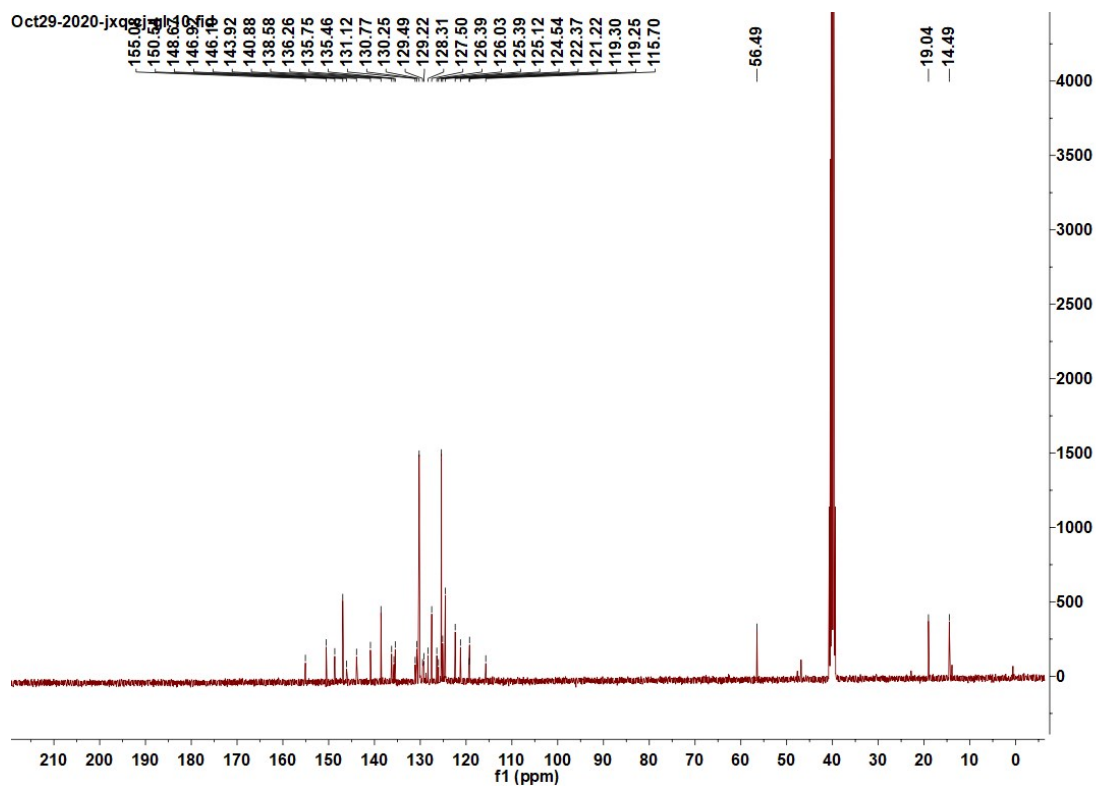**Fig. S5.** The ^1H NMR of **MPP** (600 MHz, in DMSO-d_6).

Fig. S6. ^{13}C NMR of compound **MPP** (101 MHz, in DMSO-d_6)
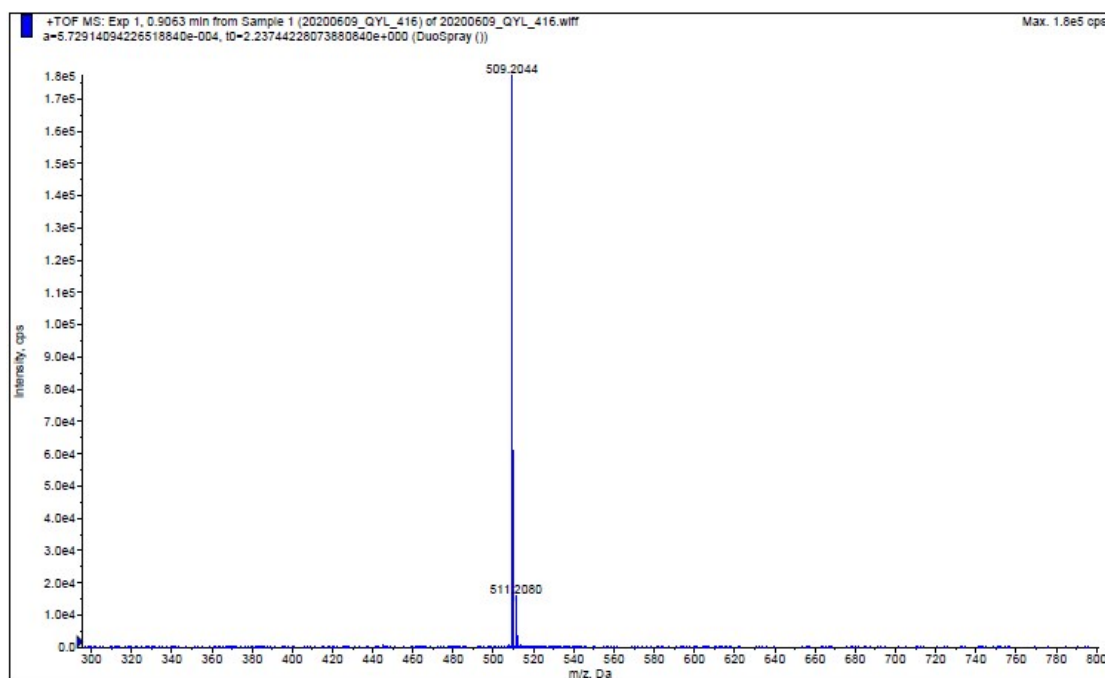
Fig. S7. ESI-MS spectrum of compound **MPP** (calculated for $C_{35}H_{29}N_2S^+$ [M+H]$^+$ 509.20, found 509.2044).
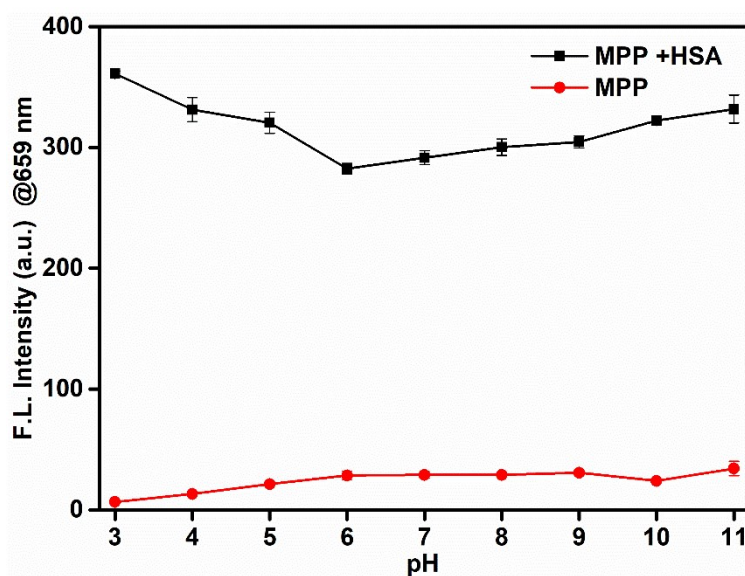
3. Photophysical properties

Fig. S8. Fluorescence intensity changes of **MPP** (10 μM) towards HSA (8 mg/mL) in PBS buffers with 1% MeCN under different pH conditions (3.0, 4.0, 5.0, 6.0, 7.0, 8.0, 9.0, 10.0, 11.0,). $\lambda_{ex}/\lambda_{em}$ = 526/659 nm.
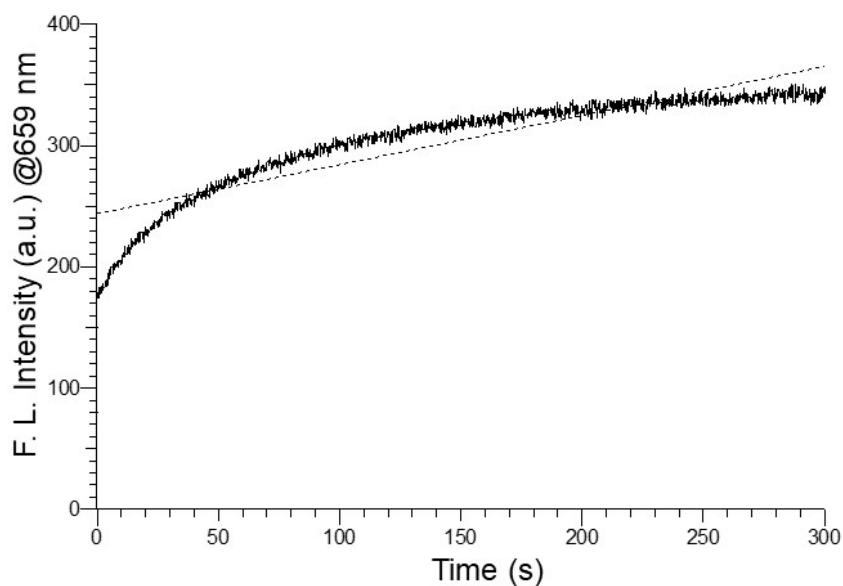
Fig. S9. Fluorescence intensity of the detecting system with incubation time.
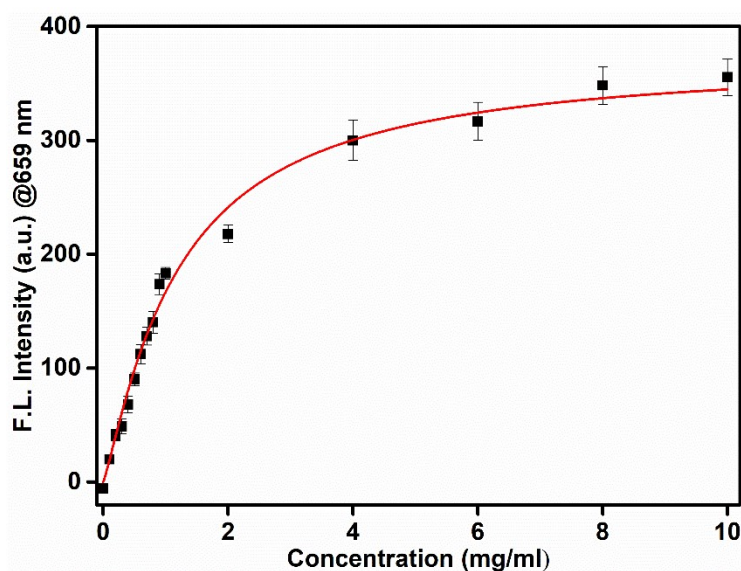

Fig. S10. Concentration-dependent changes in the fluorescence intensity of **MPP** towards HSA (0-10 mg/mL) in PBS buffers with 1% MeCN at 659 nm.
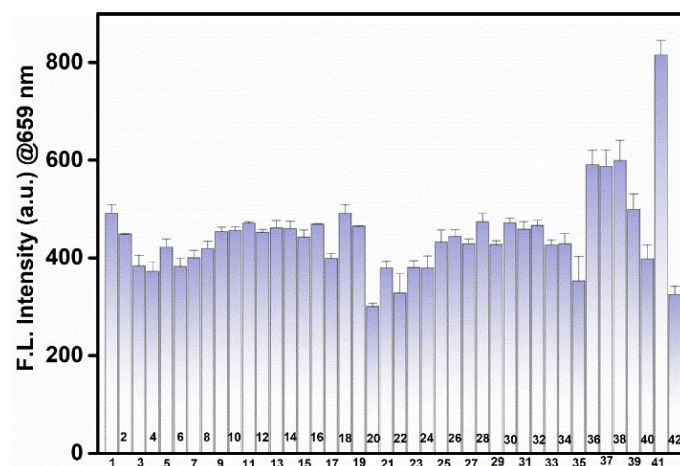

Fig. S11. Fluorescence intensity of **MPP** (10 μM) at 659 nm in the presence of HSA (8

mg/mL) after addition of various species: (1-26 (10×10^{-4} M), 27-42 (8mg/mL)): 1 = Al^{3+}, 2 = Ca^{2+}, 3 = Cr^{3+}, 4 = Cu^{2+}, 5 = Cu^{+}, 6 = Fe^{2+}, 7 = Fe^{3+}, 8 = K^{+}, 9 = Mg^{2+}, 10 = Mn^{2+}, 11 = Zn^{2+}, 12 = CH_3COO^-, 13 = Cl^-, 14 = CO_3^{2-}, 15 = F^-, 16 = HCO_3^-, 17 = HSO_3^-, 18 = HSO_4^{2-}, 19 = NO_3^-, 20 = $S_2O_3^{2-}$, 21 = SCN^-, 22 = SO_4^{2-}, 23 = ClO^-, 24 = H_2O_2, 25 = $ONOO^-$, 26 = Tyr, 27 = His, 28 = Glu, 29 = Pro, 30 = Asp, 31 = Arg, 32 = Ser, 33 = Cys, 34 = GSH, 35 = Pepsin, 36 = Trypsin, 37 = Lysozyme, 38 = Hemoglobin, 39 = RNA, 40 = DNA, 41 = BSA, 42 = HSA. All data were acquired in phosphate-buffered saline (PBS) buffer (10×10^{-3} M, pH 7.4, 1% MeCN) at 37 °C with excitation at 526 nm for 2 min, the data represent the average of three independent experiments. The error bars were ± standard deviation (SD).
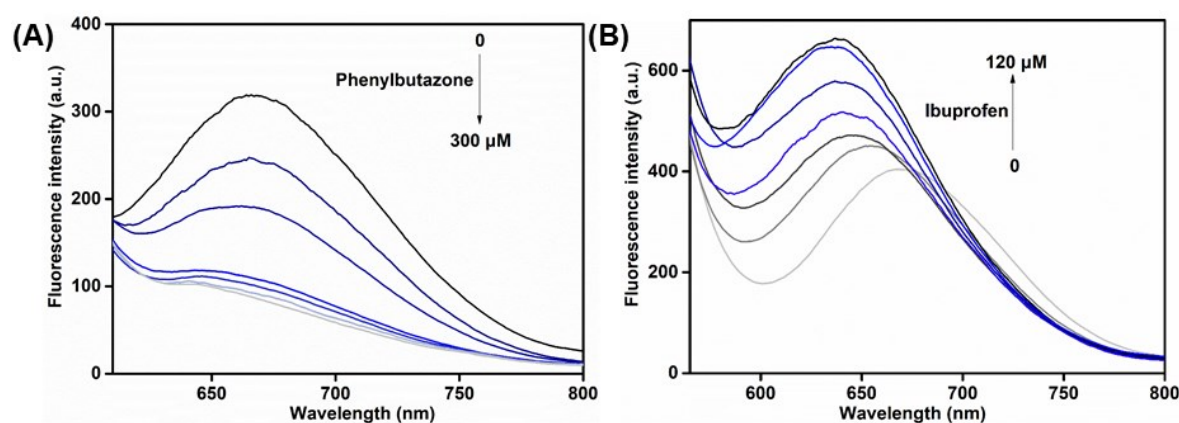

Fig. S12. Competitive displacement of the **MPP** probe in HSA by phenylbutazone (A) and ibuprofen (B). **MPP** (10 μM) was first mixed with HSA (8 mg/mL) for 5 min at 37 °C in PBS buffer to switch on fluorescent emission excited at 526 nm. Phenylbutazone and ibuprofen was then added to displace the **MPP** bound to HSA, respectively.
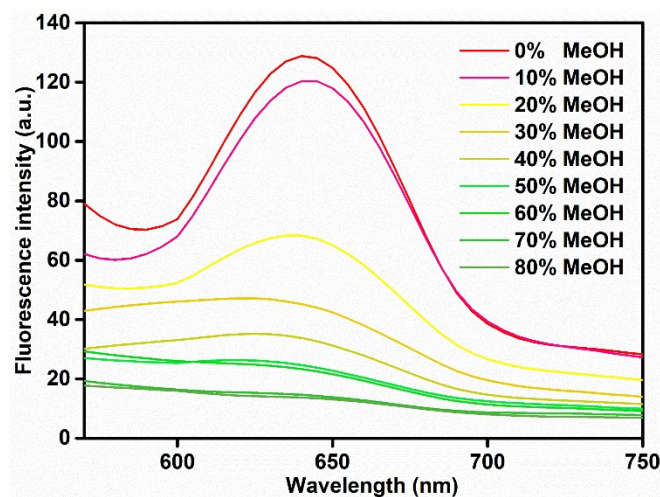

Fig. S13. Fluorescence spectra of **MPP** (10 μM) in different ratios of methanol–glycerol mixtures representing fluorescence changes with varying viscosity.
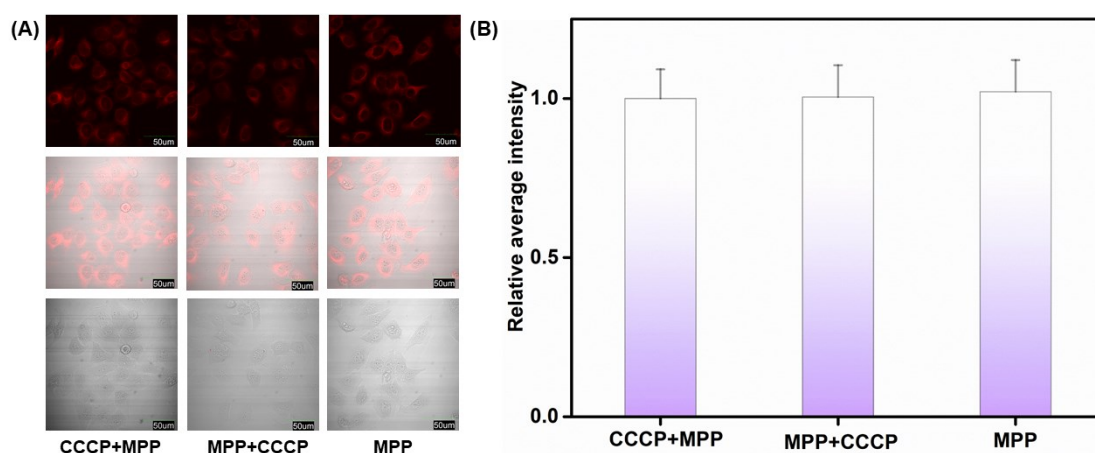
4. Bioimaging

Fig. S14. Fluorescent imaging of HeLa cells treated with **MPP** and CCCP (A). (Left panels) Cells first incubated with CCCP (20 μM) for 60 min, followed by **MPP** (4 μM) for another 60 min. (Middle panels) Cells were first incubated with **MPP** (4 μM) for 60 min, followed by CCCP (20 μM) for another 60 min. (Right panels) Cells were incubated with **MPP** (4 μM) for 60 min only. Relative average intensity of three panels (B). Scar bar = 50 μm.
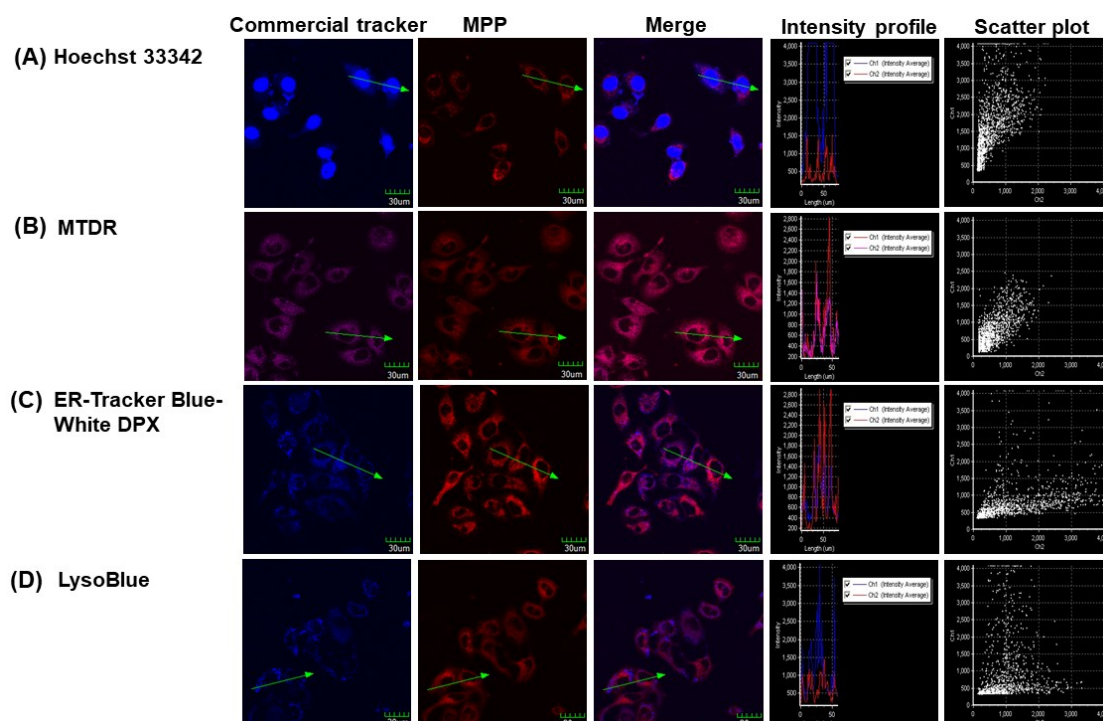

Fig. S15. Intracellular co-localization of **MPP** in HeLa cells. Live cells were treated with Hoechst 33342 (1 μM), MTDR (0.5 μM), ER-Tracker Blue-White DPX (1 μM) and LysoBlue (1 μM) for 60 min, after washing with PBS×3 times, then incubated with

MPP (10 μM) for 60 min after washing with PBS×3 times before the fluorescent images were recorded by a confocal fluorescent microscope (Olympus FV1000, 63 oil objective). Hoechst 33342 (λex = 405 nm, λem = 420-520 nm), MTDR (λex = 633 nm, λem = 680-750 nm), ER-Tracker Blue-White DPX (λex = 405 nm, λem = 430-640 nm), LysoBlue (λex = 405 nm, λem = 430-530 nm) and **MPP** fluorescence (λex = 514 nm, λem = 600-750 nm). Scale bar = 30 μm.
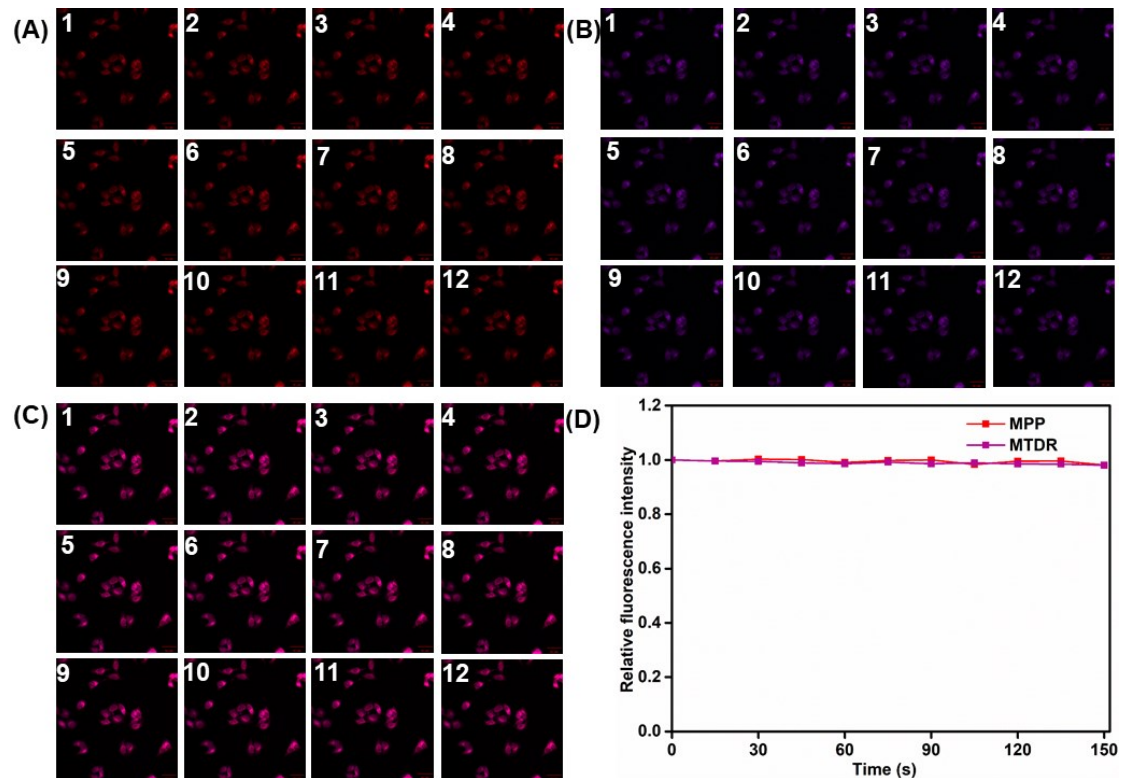

Fig. S16. Fluorescent images of **MPP** in red channel (A) and MTDR (B) in purple channel in HeLa cells under different exposure time within 150 s. (C) The merge channel of red (A) and purple (B). (D) Changes of the relative fluorescence intensity ratio versus different exposure time. Cells were pretreated with **MPP** (4 μM), subsequently, cells were imaged every 15 seconds within 150 seconds with an excitation at 514 nm for **MPP** and 633 nm for MTDR, respectively. The fluorescence images of the red channel collected at 600 - 750 nm and the purple channel collected at 680 - 750 nm. Scale bar = 50 μm.
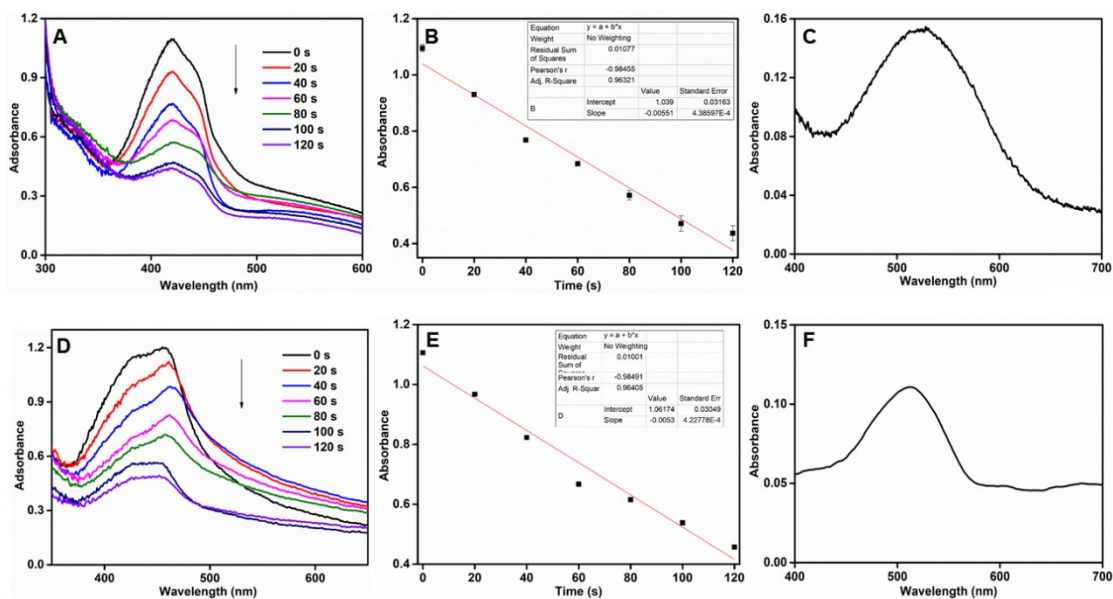
Fig. S17. (A) Schematic diagram of the basic mechanisms of photodynamic therapy. (B) The electron density distribution of frontier orbitals of **MPP**.

Fig. S18. Normalized absorbance of the DPBF solution (50 µM) at 425 nm in the presence or absence of HSA (8 mg/mL) or **MPP** (10 µM) under 526 nm laser irradiation (17 W/m^2) for different times. All the data represent the average of three independent experiments, the error bars were ± standard deviation (SD).

Fig. S19. Chemical trapping measurements of the $^{1}O_{2}$ quantum yield. (A) Photodegradation of DPBF with **MPP** (10 µM) and HSA (8 mg/mL). (B) The decomposition rate constants of DPBF by **MPP** (10 µM) and HSA (8 mg/mL). (C) The absorption peak area of **MPP** (10 µM) with HSA (8 mg/mL). (D) Photodegradation of DPBF with RB. (E) The decomposition rate constants of DPBF by RB. (F) The absorption peak area of RB.
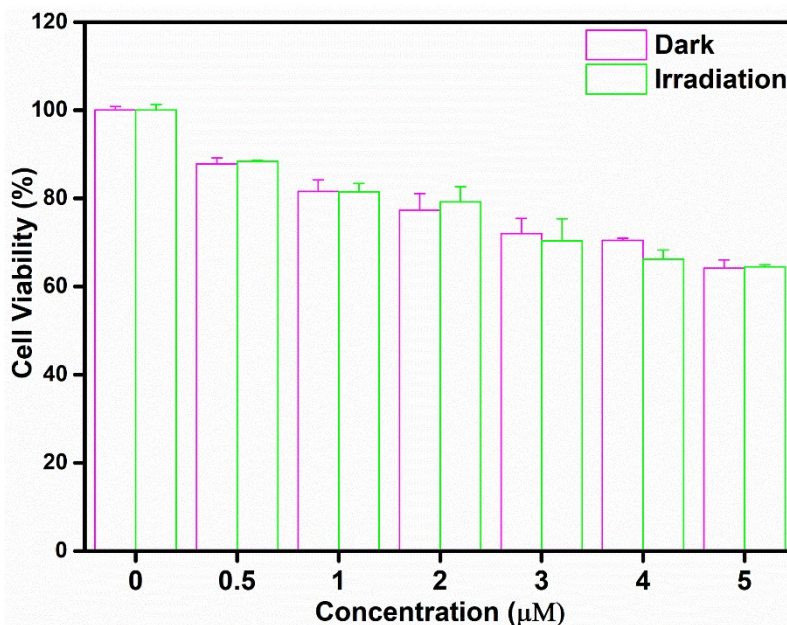

Fig. S20. Survival rates of HeLa cells stained with various concentrations of RB with or without green light illumination for 10 min.
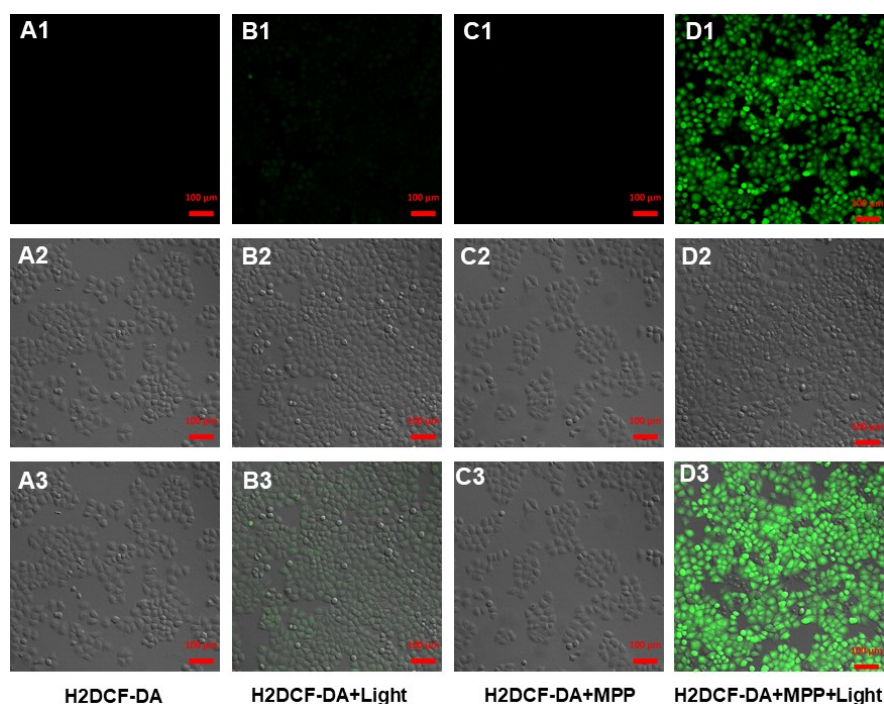
Fig. S21. Confocal fluorescence imaging of intracellular ROS in HeLa cells using H2DCF-DA (10 µM) and **MPP** (4 µM) upon diverse treatments. λex = 488 nm. λem = 500 - 550 nm. Scale bar = 100 µm.
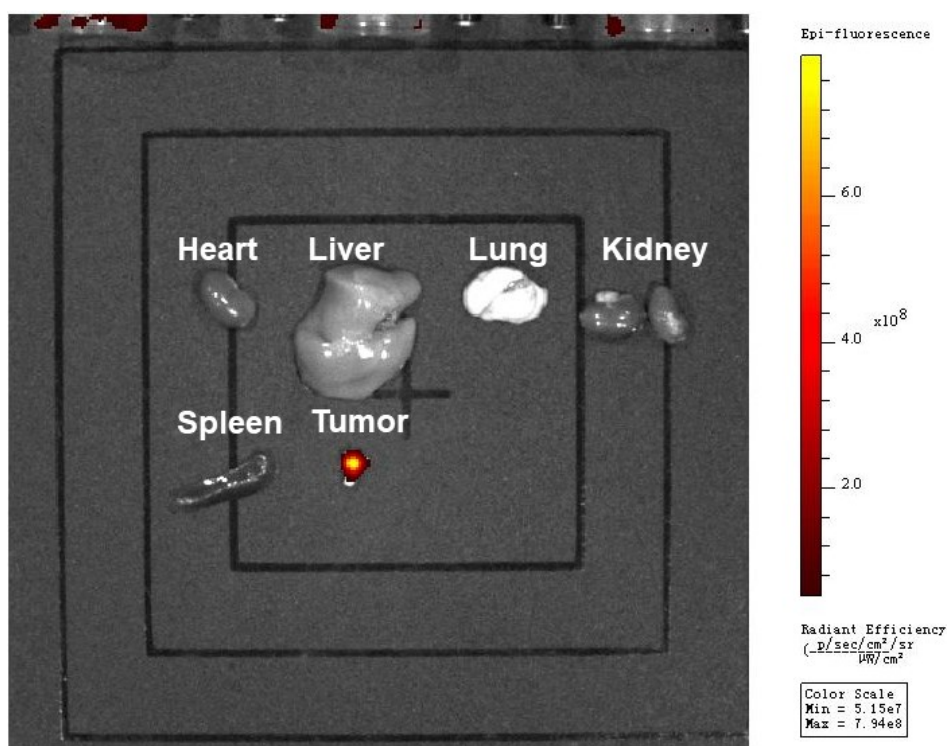

Fig. S22. *Ex vivo* fluorescence imaging of various organs and tumor tissue from mice after intratumoral injection of **MPP** (10 µM, 200 µL). The mice were sacrificed at 24 h post-injection.

Table S1. The vertical excitation (UV-Vis absorption) energies, oscillator strengths,

and assignments calculated using TDDFT at B3LYP/6-311G (d) level.

Excited states	Energy(eV)/λ(nm)	f	Composition
S0-S1	1.853/669	1.0752	H→L (100%)
S0-S2	2.771/447	0.0975	H-1→L (91%)
S0-T1	1.374/902	0.0000	H→L (83%)
S0-T2	2.151/576	0.0000	H-1→L (75%)
S0-T3	2.512/494	0.0000	H→ L+1 (68%)

References

1   Y. Lu, B. Peng, X. Qiu, X. Li, Z. Li, D. Zhang, W. Ji, B. Fang, Q. Wu, C. Zhang, L. Li and W. Huang, Mater. Adv., 2020, 1, 1448–1454.

2   Gaussian 16, Revision A.03, M. J. Frisch, G. W. Trucks, H. B. Schlegel, G. E. Scuseria, M. A. Robb, J. R. Cheeseman, G. Scalmani, V. Barone, G. A. Petersson, H. Nakatsuji, X. Li, M. Caricato, A. V Marenich, J. Bloino, B. G. Janesko, R. Gomperts, B. Mennucci, H. P. Hratchian, J. V Ortiz, A. F. Izmaylov, J. L. Sonnenberg, D. Williams-Young, F. Ding, F. Lipparini, F. Egidi, J. Goings, B. Peng, A. Petrone, T. Henderson, D. Ranasinghe, V. G. Zakrzewski, J. Gao, N. Rega, G. Zheng, W. Liang, M. Hada, M. Ehara, K. Toyota, R. Fukuda, J. Hasegawa, M. Ishida, T. Nakajima, Y. Honda, O. Kitao, H. Nakai, T. Vreven, K. Throssell, J. A. Montgomery Jr., J. E. Peralta, F. Ogliaro, M. J. Bearpark, J. J. Heyd, E. N. Brothers, K. N. Kudin, V. N. Staroverov, T. A. Keith, R. Kobayashi, J. Normand, K. Raghavachari, A. P. Rendell, J. C. Burant, S. S. Iyengar, J. Tomasi, M. Cossi, J. M. Millam, M. Klene, C. Adamo, R. Cammi, J. W. Ochterski, R. L. Martin, K. Morokuma, O. Farkas, J. B. Foresman and D. J. Fox, Gaussian, Inc., Wallingford CT, 2016.

3   C. Shao, J. Yuan, Y. Liu, Y. Qin, X. Wang, J. Gu, G. Chen, B. Zhang, H.-K. Liu, J. Zhao, H.-L. Zhu and Y. Qian, Proc. Natl. Acad. Sci., 2020, 117, 10155–10164.

4   X. Xue, C. Qian, H. Fang, H. Liu, H. Yuan, Z. Guo, Y. Bai and W. He, Angew. Chemie Int. Ed., 2019, 58, 12661–12666.

5   Y. Yuan, C. J. Zhang, S. Xu and B. Liu, Chem. Sci., 2016, 7, 1862–1866.

6   Y.-L. Qi, L.-L. Chen, L. Guo, C. Shao, Y. Liu, Y.-S. Yang, Z.-X. He and H.-L. Zhu, Chem. – An Asian J., 2020, 15, 3551–3557.